Loudspeaker Voice-Coil Inductance Losses: Circuit Models, Parameter Estimation, and Effect on Frequency Response

W. Marshall Leach, Jr., Professor
Georgia Institute of Technology
School of Electrical and Computer Engineering
Atlanta, Georgia 30332-0250 USA

Abstract— **When the series resistance is separated and treated as a separate element, it is shown that losses in an inductor require the ratio of the flux to mmf in the core to be frequency dependent. For small-signal operation, this dependence leads to a circuit model composed of a lossless inductor and a resistor in parallel, both of which are frequency dependent. Mathematical expressions for these elements are derived under the assumption that the ratio of core flux to mmf varies as ω^{n-1}, where n is a constant. A linear regression technique is described for extracting the model parameters from measured data. Experimental data are presented to justify the model for the lossy inductance of a loudspeaker voice coil. A SPICE example is presented to illustrate the effects of voice-coil inductor losses on the frequency response of a typical driver.**

I. Introduction

For small-signal operation, the voice coil of an electrodynamic loudspeaker driver can be modeled by three elements in series – a resistance, a lossy inductance, and a dependent voltage source representing the back emf generated when the diaphragm moves [1]. The circuit is shown in Fig. 1, where R_E is the resistance and L_E is the inductance. The back emf is given by $B\ell u_D$, where B is the magnetic flux in the air gap, ℓ is the effective length of wire that cuts the flux, and u_D is the mechanical velocity of the diaphragm. The back emf due to the diaphragm motion exhibits a band-pass effect that decreases toward zero as frequency is increased above the fundamental resonance frequency of the driver. At the higher frequencies, the impedance is dominated by the inductance.

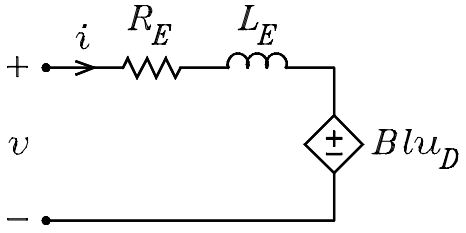

Fig. 1. Equivalent voice-coil circuit.

When the series resistance of the voice coil is separated and treated as a separate element, the lossy inductance can be modeled at any frequency by a circuit consisting of a lossless inductor in parallel with a resistor [2]. If the frequency is changed, the values of both the inductor and the resistor change. In [3], it is shown that eddy current losses in the magnet structure cause the impedance of the lossy inductor to be of the form $Z = K\sqrt{j\omega}$. In [4], experimental data is presented which shows that this model fails to predict the high-frequency impedance of many drivers. An empirical model is described for which the impedance of the lossy inductor is assumed to be of the form $Z = K_r\omega^{X_r} + jK_i\omega^{X_i}$. An experimental method for determining the model parameters is described that is based on impedance measurements at two frequencies.

The lossy inductance model of [3] requires one parameter. The model of [4] requires four. In the following, a model is derived which requires two parameters. A linear regression method for determining these from measured voice-coil impedance data is developed and an example is presented. A SPICE model for the lossy inductor is described and a SPICE simulation is used to illustrate the effect of the inductor losses on the frequency response of a driver.

II. Inductor Fundamentals

The analysis presented here assumes an inductor that is wound with wire that exhibits zero resistance. When the analysis is applied to the lossy inductance of a loudspeaker voice coil, it is assumed that the series resistance of the voice coil has been separated and is treated as a separate element. Although both the large-signal and small-signal behaviors of inductors are reviewed in this section, the model developed for the lossy inductor is strictly valid only for small-signal operation.

Figure 2 illustrates an inductor consisting of turns of wire wound on a rectangular core. The total flux λ linking the coil is given by $\lambda = N\varphi$, where N is the number of turns of wire and φ is the flux linking a single turn. The voltage across the coil is given by

$$v = \frac{d\lambda}{dt} = N\frac{d\varphi}{dt} \tag{1}$$

The magnetic properties of the core material determine the relationship between the current in the coil and the impressed voltage. These properties are usually described by a plot of the flux φ versus the impressed magnetomotive force or mmf

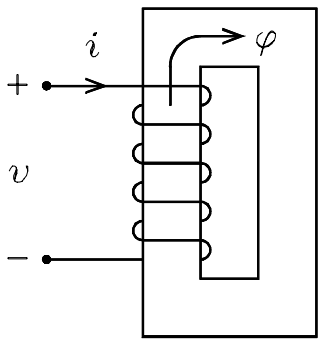

Fig. 2. Inductor consisting of N turns of zero-resistance wire wound on a magnetic core.

given by $F = Ni$, where i is the current in the coil. Two such plots are shown in Fig. 3(a), where it is assumed that the mmf varies sinusoidally with time and has a mean value of zero. The arrows indicate the direction of motion around the curves as time increases. Curve 1 assumes the core material is linear. In this case, the curve is an ellipse. For a lossless core, the ellipse degenerates into a straight line. All magnetic materials exhibit a nonlinearity that causes the flux to exhibit a saturation effect as the impressed mmf is increased above some value. Such a plot is shown in curve 2, where the flux is assumed to saturate at $1/2$ of the peak value in curve 1. The curves are often referred to as hysteresis loops.

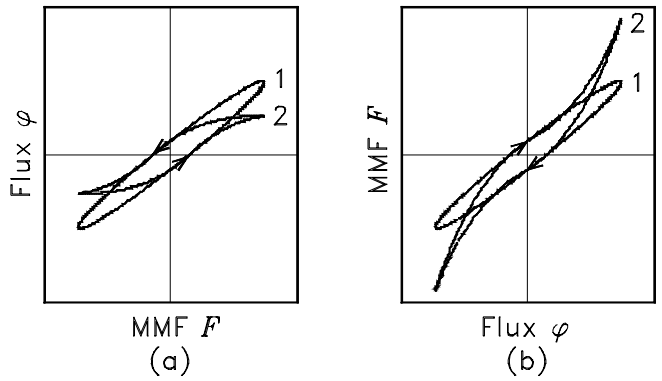

Fig. 3. (a) Plots of flux versus mmf. (b) Plots of mmf versus flux.

The curves in Fig. 3(a) assume that the mmf is the independent variable. Because $F = Ni$, it follows that the curves are plotted for a current source excitation. If a sinusoidal voltage is impressed across the coil, it follows from Eq. (1) that the flux linking each turn is determined by the voltage. Thus the flux is the independent variable for a voltage source excitation. In this case, the plots of F versus φ are shown in Fig. 3(b). Curve 1 for a linear core material remains an ellipse. However, curve 2 for a core material that exhibits flux saturation effects shows a rapidly increasing mmf as the flux is increased. For the assumed flux saturation factor of $1/2$, the peak value of the mmf is twice the peak value in curve 1.

Figure 4 illustrates the voltage, flux, and current waveforms for a sinusoidal voltage impressed across the coil. The current i_1 is for the linear core. The flux lags the impressed voltage by 90^{o}. The current lags the voltage by less than 90^{o}, increasing to 90^{o} for a lossless core. The current i_2 is for the nonlinear core. The current waveform is no longer sinusoidal. It exhibits a peak value that is higher by a factor of 2. An increase in the applied voltage causes this peak to increase rapidly, causing the inductor to approach a short circuit as the core saturates.

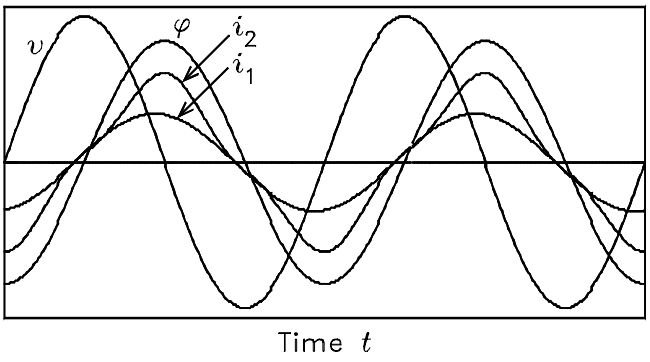

Fig. 4. Plots of voltage v, flux φ, current i_1 for the linear core, and current i_2 for the nonlinear core versus time.

In the following, a linear magnetic material is assumed. Otherwise, the definition of inductance would be impossible and phasor analyses would be precluded. For a linear core, the phasor form of Eq. (1) is

$$V = j\omega N\varphi = j2\pi f N\varphi \tag{2}$$

where $\omega = 2\pi f$ is the radian frequency. For $|V|$ a constant, it can be seen that $|\varphi|$ is inversely proportional to the product $f \times N$. It follows that any effects of core saturation are reduced if the frequency of the impressed voltage is increased or if the number of turns of wire is increased. This result plays an important role in transformer design if core saturation problems are to be avoided. The lower the frequency of operation, the more turns of wire must be used, causing low-frequency transformers to be larger than high-frequency counterparts. It also explains why a "step-down" transformer cannot be used in reverse, i.e. with the primary and secondary reversed.

For a linear magnetic material, a sinusoidal voltage impressed across the coil results in sinusoidal current, flux, and mmf. Let the flux and mmf be given by

$$\varphi(t) = \varphi_1 \cos\omega t = \mathrm{Re}\left[\varphi_1 \exp(j\omega t)\right] \tag{3}$$

$$F(t) = F_1 \cos(\omega t + \theta) = \mathrm{Re}\left[F_1 \exp(j\theta)\exp(j\omega t)\right] \tag{4}$$

where θ is the angle by which the mmf leads the flux, or alternately the angle by which the flux lags the mmf. In general, θ is a function of the frequency ω. The corresponding voltage and current are given by

$$\begin{aligned} v(t) &= N\frac{d\varphi(t)}{dt} \\ &= -\omega N\varphi_1 \sin\omega t \\ &= \mathrm{Re}\left[j\omega N\varphi_1 \exp(j\omega t)\right] \end{aligned} \tag{5}$$

$$\begin{aligned} i(t) &= \frac{1}{N}F(t) \\ &= \frac{F_1}{N}\cos(\omega t+\theta) \\ &= \mathrm{Re}\left[\frac{F_1}{N}\exp(j\theta)\exp(j\omega t)\right] \end{aligned} \tag{6}$$

It follows that the phasor voltage and current, respectively, are given by

$$V = j\omega N\varphi_1 \tag{7}$$

$$I = \frac{F_1}{N}\exp(j\theta) = \frac{F_1}{N}(\cos\theta + j\sin\theta) \tag{8}$$

For a constant impressed voltage, the current in the coil is proportional to the admittance $Y(j\omega)$ given by

$$\begin{aligned} Y(j\omega) &= \frac{I}{V} \\ &= \frac{F_1}{j\omega N^2\varphi_1}\exp(j\theta) \\ &= \frac{F_1}{N^2\varphi_1}\left(\frac{\sin\theta}{\omega} - j\frac{\cos\theta}{\omega}\right) \end{aligned} \tag{9}$$

It follows that the equivalent circuit of the inductor can be represented as a parallel resistor and inductor given by

$$R = \frac{\omega N^2\varphi_1}{F_1\sin\theta} \tag{10}$$

$$L = \frac{N^2\varphi_1}{F_1\cos\theta} \tag{11}$$

Because R and L must be positive, it can be seen that the angle θ must satisfy the condition $0 \le \theta \le 90^{\circ}$. These equations are used in the following as the basis for the circuit model for the lossy inductance of a loudspeaker voice coil. The key in the development of the model is the frequency dependence of the ratio of flux to mmf in the core, i.e. in the frequency dependence of φ_1/F_1.

III. The Lossy Inductor Model

The author teaches a senior elective audio engineering course at Georgia Tech where students are required to bring a loudspeaker driver into the laboratory and measure its small-signal parameters. After the acquisition of equipment that provided the capability of making detailed automated measurements of voice-coil impedance at high frequencies, it was noticed that the phase of the impedance of drivers approached a constant at high frequencies after the series resistance of the coil and the motional impedance term are subtracted. For a lossless voice-coil inductance, this phase should be 90°. However, experimentally observed values were usually in the 60° to 70° range. By coincidence, it was observed that the phase could be predicted from the slope of the log-log plot of the magnitude of the impedance versus frequency. This slope, when multiplied by 90°, predicted the phase. This interesting and puzzling relationship was explained when the author remembered Bode's gain-phase integral [5] from an undergraduate course in control systems. This ingenious integral is the basis of the lossy inductor model that is described in this section.

By Eq. (9), the admittance of the lossy inductor has a magnitude and phase given by

$$|Y(j\omega)| = \sqrt{Y(j\omega)Y^*(j\omega)} = \frac{F_1}{\omega N^2\varphi_1} \tag{12}$$

$$\begin{aligned} \beta &= \arg[Y(j\omega)] \\ &= \tan^{-1}\left\{\frac{\mathrm{Im}[Y(j\omega)]}{\mathrm{Re}[Y(j\omega)]}\right\} \\ &= \theta - \frac{\pi}{2} \end{aligned} \tag{13}$$

If the ratio of φ_1 to F_1 is independent of frequency, it can be seen that $|Y(j\omega)|$ is inversely proportional to ω. In this case, the slope of the plot of $\ln|Y(j\omega)|$ versus $\ln(\omega)$ is -1.

Because there is no evidence that a two-terminal passive lumped element network can have an admittance or impedance transfer function that is not minimum phase, it will be assumed here that $Y(j\omega)$ represents a minimum-phase transfer function. In this case, the phase β is related to the magnitude by Bode's gain-phase integral

$$\beta = \frac{1}{\pi}\int_{-\infty}^{\infty}\frac{d\alpha}{du}\ln\left(\coth\left|\frac{u}{2}\right|\right)du \tag{14}$$

where $\alpha = \ln|Y(j\omega)|$ and $u = \ln(\omega)$. For the case $\varphi_1/F_1 =$ a constant, $|Y(j\omega)| \propto 1/\omega$ in Eq. (12), and it follows that $d\alpha/du = -1$. In this case, Bode's integral predicts $\beta = -\pi/2$, where the relation

$$\int_{-\infty}^{\infty}\ln\left(\coth\left|\frac{u}{2}\right|\right)du = \frac{\pi^2}{2} \tag{15}$$

has been used. By Eq. (13), $\beta = -\pi/2$ results in $\theta = 0$. Thus by Eqs. (10) and (11), R is an open circuit and L is a constant. In this case, the inductor is lossless. It follows that losses require the ratio of flux to mmf to be frequency dependent.

For a lossy inductor, the most general model for the frequency dependence of the ratio of flux to mmf is a power series in ω. To model an impedance which has a phase that is independent of frequency, it follows from Bode's integral that the power series must have only one term. It is assumed here that $\varphi_1/F_1 = K\omega^{n-1}/N^2$, where n and K are constants. It has been observed that this choice leads to excellent agreement with experimental data and an example is presented in the following which illustrates this. In this case, it follows from Eq. (12) that $|Y(j\omega)| = 1/(K\omega^n)$ so that $d\alpha/du = -n$ and Bode's integral predicts $\beta = -n\pi/2$. By Eq. (13), this results in $\theta = (1-n)\pi/2$. Thus, Eq. (9) for $Y(j\omega)$ can be written

$$\begin{aligned} Y(j\omega) &= \frac{1}{j\omega K\omega^{n-1}}\exp\left[j\frac{(1-n)\pi}{2}\right] \\ &= \frac{1}{(j\omega)^n K} \\ &= \frac{1}{K\omega^n}\left[\cos\left(\frac{n\pi}{2}\right) - j\sin\left(\frac{n\pi}{2}\right)\right] \end{aligned} \tag{16}$$

It follows that the equivalent circuit of the inductor consists of a parallel resistor R_p and inductor L_p given by

$$R_p = \frac{K\omega^n}{\cos(n\pi/2)} \tag{17}$$

$$L_p = \frac{K\omega^{n-1}}{\sin(n\pi/2)} \tag{18}$$

For both R_p and L_p to be positive, n must satisfy $0 \leq n \leq 1$. For $n = 1$, $R_p = \infty$ and L_p is independent of ω. For $n = 0$, $L_p = \infty$ and R_p is independent of ω. It can be concluded that the losses increase as n decreases, causing the inductor to change from a lossless inductor into a resistor as n decreases from 1 to 0. The equivalent circuit of the inductor is shown in Fig. 5(a).

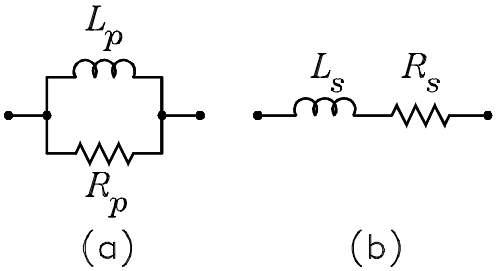

Fig. 5. Equivalent circuits of the lossy inductor. (a) Parallel model. (b) Series model.

From Eq. (9), it follows that the impedance of the lossy inductor is given by

$$\begin{aligned} Z(j\omega) &= \frac{1}{Y(j\omega)} \\ &= K(j\omega)^n \\ &= K\omega^n\left[\cos\left(\frac{n\pi}{2}\right) + j\sin\left(\frac{n\pi}{2}\right)\right] \end{aligned} \tag{19}$$

Thus the equivalent circuit can also be represented by a series resistor R_s and inductor L_s given by

$$R_s = K\omega^n \cos\left(\frac{n\pi}{2}\right) \tag{20}$$

$$L_s = K\omega^{n-1}\sin\left(\frac{n\pi}{2}\right) \tag{21}$$

For $n = 1$, $R_s = 0$ and L_s is independent of ω. For $n = 0$, $L_s = 0$ and R_s is independent of ω. The series equivalent circuit of the inductor is shown in Fig. 5(b). For $n = 1/2$, the expression for $Z(j\omega)$ reduces to the one derived in [3]. For this case, the real and imaginary parts of $Z(j\omega)$ are equal and vary as $\sqrt{\omega}$.

For a sinusoidal flux having a peak amplitude φ_1, the peak amplitude of the impressed voltage is $\omega N\varphi_1$. The average power dissipated in the inductor is thus given by

$$\begin{aligned} P &= \frac{(\omega N\varphi_1)^2}{2R_p} \\ &= \frac{(N\varphi_1)^2\cos(n\pi/2)}{2K}\omega^{2-n} \end{aligned} \tag{22}$$

As an example, Fig. 6 shows a log-log plot of experimental transformer core loss data given in [6] for losses in laminated silicon steel for a constant impressed flux at four frequencies. The straight line approximation to the data has a slope of 1.24. For this case, it follows that $n = 2 - 1.24 = 0.76$. Although the range of frequencies for the data was much lower than the range of interest in loudspeaker drivers, this value of n is close to values observed by the author for some drivers. In particular, it corresponds exactly to the value measured for one sample of an 18 inch JBL model 2241H Professional Series driver.

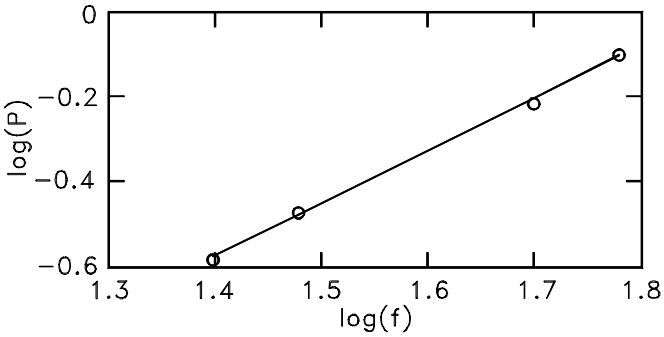

Fig. 6. Plot of $\log(P)$ versus $\log(f)$ for experimental transformer core loss data presented in [6].

Although the parallel model corresponds to the traditional model for a lossy inductor, the series and parallel models are equivalent. The parameters K and n for a driver can be obtained from measured voice-coil impedance or admittance data. The method described in the following uses impedance data.

IV. Inductor Parameter Estimation

In general, the voice-coil impedance of a driver on an infinite baffle can be written [7]

$$\begin{aligned} Z_{VC}(s) &= R_E + Z_L(s) \\ &\quad + \frac{R_{ES}(1/Q_{MS})(s/\omega_S)}{(s/\omega_S)^2 + (1/Q_{MS})(s/\omega_S) + 1} \end{aligned} \tag{23}$$

where $s = j\omega$, R_E is the voice-coil resistance, $Z_L(s)$ is the impedance of the lossy inductor, ω_S is the fundamental resonance frequency of the driver, Q_{MS} is its mechanical quality factor, and R_{ES} is the amount by which the impedance peaks up at resonance. The procedure described in the following for determining n and K assumes that R_E, R_{ES}, ω_S, and Q_{MS} are known.

It follows from Eq. (23) that the lossy inductor impedance $Z_L(j\omega)$ can be written

$$\begin{aligned} Z_L(j\omega) &= Z_{VC}(j\omega) - R_E \\ &\quad - \frac{R_{ES}(1/Q_{MS})(j\omega/\omega_S)}{(j\omega/\omega_S)^2 + (1/Q_{MS})(j\omega/\omega_S) + 1} \end{aligned} \tag{24}$$

The natural logarithms of $Z_L(j\omega)$ and the model impedance $Z(j\omega)$ given by Eq. (19), respectively, are given by

$$\ln[Z_L(j\omega)] = \ln|Z_L(j\omega)| + j\arg[Z_L(j\omega)] \tag{25}$$

$$\ln[Z(j\omega)] = \ln(K) + n\ln(\omega) + j\frac{n\pi}{2} \tag{26}$$

If $\ln[Z_L(j\omega)]$ is known over a band of frequencies for a particular driver and the parameters n and K can be determined

such that $\ln[Z(j\omega)] - \ln[Z_L(j\omega)] = 0$ over that band, then $Z(j\omega)$ is an exact model for the inductor impedance over the band. A method for determining n and K that minimizes the mean magnitude-squared difference between the functions is described below.

Let $Z_{VC}(j\omega)$ be measured at a set of N frequencies and the value of $Z_L(j\omega)$ calculated for each. An error function ϵ can be defined as follows:

$$\begin{aligned}\epsilon &= \sum_i \left| \ln[Z(j\omega_i)] - \ln[Z_L(j\omega_i)] \right|^2 \\ &= \sum_i \left\{ \left[\ln(K) + n\ln(\omega_i) - \ln|Z_L(j\omega_i)| \right]^2 \right. \\ &\quad \left. + \left[\frac{n\pi}{2} - \arg[Z_L(j\omega_i)] \right]^2 \right\} \end{aligned} \quad (27)$$

For minimum error between the measured impedance and the model impedance, the conditions $\partial\epsilon/\partial n = 0$ and $\partial\epsilon/\partial[\ln(K)] = 0$ must hold. These conditions lead to the solutions

$$\begin{aligned} n &= \frac{1}{\Delta}\left[\sum_i \ln|Z_L(j\omega_i)| \ln(\omega_i) \right. \\ &\quad -\frac{1}{N}\sum_i \ln|Z_L(j\omega_i)| \times \sum_i \ln(\omega_i) \\ &\quad \left. +\frac{\pi}{2}\sum_i \arg[Z_L(j\omega_i)] \right] \end{aligned} \quad (28)$$

$$\ln(K) = \frac{1}{N}\left[\sum_i \ln|Z_L(j\omega_i)| - n\sum_i \ln(\omega_i) \right] \quad (29)$$

where Δ is given by

$$\Delta = \sum_i [\ln(\omega_i)]^2 - \frac{1}{N}\left[\sum_i \ln(\omega_i) \right]^2 + N\left(\frac{\pi}{2}\right)^2 \quad (30)$$

When these equations are satisfied, the curves of the magnitude and phase of the model impedance $Z(j\omega)$ fit those of the measured impedance $Z_L(j\omega)$ in a minimum mean-squared error sense. Note that the error is simultaneously minimized for a log-log plot of $|Z_L(j\omega)|$ and a linear-log plot of the phase of $Z_L(j\omega)$. The above equations are used in the following section to illustrate an application of the lossy inductor model to an example driver.

V. A Numerical Example

The driver selected for this example is the Eminence model 10290. This is a 10 inch driver having a 38 ounce magnet and an accordion suspension. Its measured parameters are $R_E = 5.08\ \Omega$, $f_S = 35.2$ Hz, $R_{ES} = 32.0\ \Omega$, and $Q_{MS} = 2.80$. Fig. 7 shows plots of the measured values of $\mathrm{Re}[Z_{VC}(j\omega) - R_E]$ and the calculated values of $\mathrm{Re}[Z_L(j\omega)]$ defined in Eq. (24). Fig. 8 shows corresponding plots of $\mathrm{Im}[Z_{VC}(j\omega) - R_E]$ and $\mathrm{Im}[Z_L(j\omega)]$. In the region around the resonance frequency, some ripple in the curves for $Z_L(j\omega)$ is evident. While some of this can be attributed to random measurement errors and loss of precision when close numbers are subtracted, a major cause is probably the somewhat crude model for $Z_{VC}(j\omega)$ in Eq. (23) used to calculate $Z_L(j\omega)$. For example, R_{ES} is not a constant, in general. In addition, suspension creep most likely affects the fit of the model impedance around resonance. Also frequency dependence of the suspension compliance and resistance make it difficult to estimate or even define a precise resonance frequency.

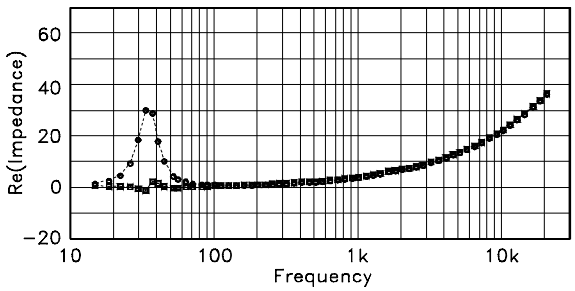

Fig. 7. Linear-log plots of $\mathrm{Re}[Z_{VC}(j2\pi f) - R_E]$ (circles) and $\mathrm{Re}[Z_L(j2\pi f)]$ (boxes) versus frequency.

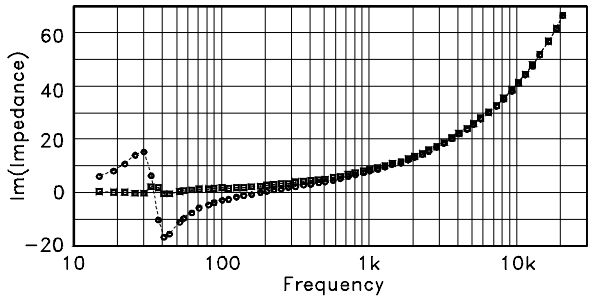

Fig. 8. Linear-log plots of $\mathrm{Im}[Z_{VC}(j2\pi f) - R_E]$ (circles) and $\mathrm{Im}[Z_L(j2\pi f)]$ (boxes) versus frequency.

The frequency range chosen for determination of n and K from the measured data was the range from 2 kHz to 20 kHz. This region was chosen to minimize the effect on the calculations of a "jog" in the measured phase below 2 kHz. There were 21 measurement points in the range. With the assistance of Mathcad, the values obtained from Eqs. (28) through (30) were $n = 0.688$ and $K = 0.0235$. Figs. 9 and 10 show the measured magnitude and phase of the impedance $Z_L(j\omega)$ in this range plotted as circles and those calculated from Eq. (19) plotted as solid lines. The magnitude approximation shows excellent agreement with the measured values. The measured phase values exhibit a slight ripple about the calculated value of 62°, some of which is likely a remnant of the "jog" in the phase below 2 kHz. The rms phase deviation is 0.66°, or just over 1%, a figure which statistically indicates excellent agreement.

Figures 11 and 12 show the magnitude and phase of the measured impedance and the magnitude and phase predicted by Eq. (23) for the frequency range from 15 Hz to 20 kHz. The measured values are plotted as circles and the calculated values as solid lines. The figures show excellent agreement between the measured values and the values predicted by the model equa-

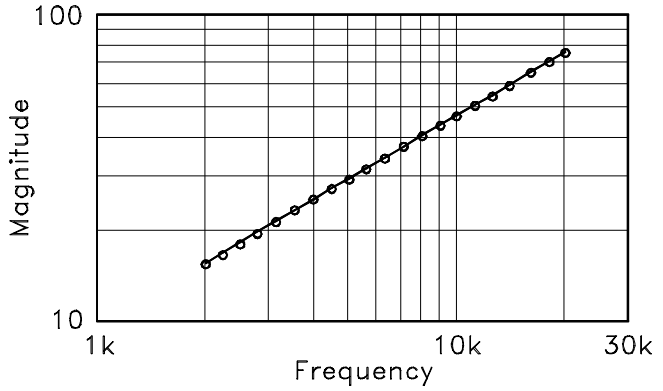

Fig. 9. Log-log plots of the calculated $|Z_L|$ (circles) and the approximating function (solid line) versus frequency for the range 2 kHz to 20 kHz.

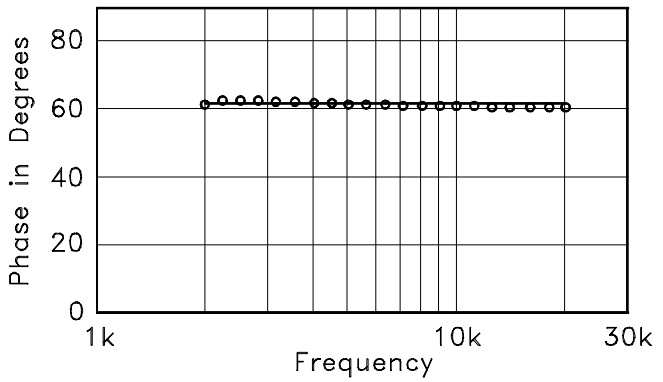

Fig. 10. Linear-log plots of the calculated phase of Z_L (circles) and the approximating function (solid line) versus frequency for the range 2 kHz to 20 kHz.

tions. Indeed, examination of the figures shows better agreement in the high-frequency range where the impedance of the inductor dominates. Examination of Fig. 12 shows a rising asymptotic behavior in the high-frequency phase whereas Fig. (10) exhibits a constant phase. This difference is caused by the phase of the motional impedance of the voice-coil, which is subtracted out in Fig. 10. Above the fundamental resonance frequency, the phase of the motional impedance is negative, approaching zero as frequency is increased, thus causing the rising behavior in the high-frequency phase in Fig. 12. The latter figure shows the "jog" in the phase between 1.4 and 1.6 kHz which is not shown in Fig. 10. This is because the points chosen for Fig. 10 were in the range from 2 kHz to 20 kHz.

The author has had a great deal of experience with student projects involving loudspeaker measurements and has found the lossy inductor model described here to give excellent results. It is felt that the "jog" in the phase in Fig. 12 between 1.4 and 1.6 kHz was due to a resonance effect in the diaphragm and that it was responsible for the slight ripple observed in Fig. 10. The experimental data shown here were measured with a MLSSA analyzer. A repeat of the measurements with an Audio Precision System II analyzer showed an almost identical behavior. Similar "jogs" in the measured phase have been observed with many drivers. Indeed, some drivers exhibit multiple "jogs" in the phase response, some of which are pronounced.

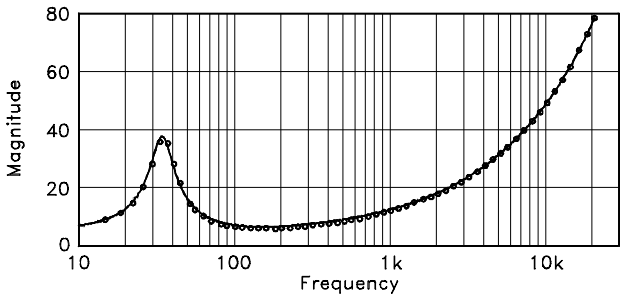

Fig. 11. Linear-log plots of the measured $|Z_{VC}|$ (circles) and the approximating function (solid line) versus frequency.

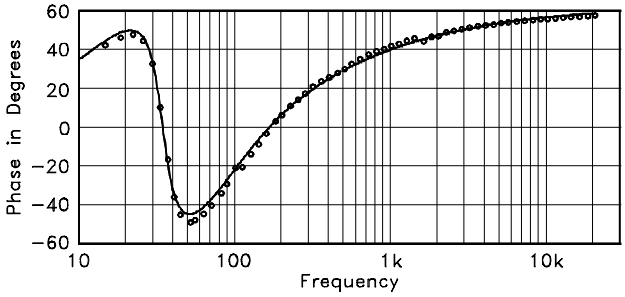

Fig. 12. Linear-log plots of the measured phase of Z_{VC} (circles) and the approximating function (solid line) versus frequency.

VI. A SPICE Model and Simulation Example

A SPICE model for the lossy inductor is described in this section and a simulation of a closed-box woofer system is presented to illustrate the effect of the inductor losses on the frequency response of a driver. Fundamentals of SPICE simulations of loudspeaker systems are covered in [1] and [8]. Fig. 13 shows a voltage controlled current source connected between nodes labeled `N1` and `N2`. If the current through the source is equal to the voltage across it divided by the impedance of the lossy inductor given by Eq. (19), then the source simulates the inductor. The analog behavioral modeling feature of *PSpice* can be used to implement this operation with the line

`GZE N1 N2 LAPLACE {V(N1,N2)}={1/(`K`*PWR(S,`n`))}`

where numerical values must be used for K and n.

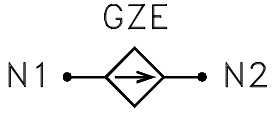

Fig. 13. SPICE model for the lossy inductor.

The SPICE circuit for the simulation is shown in Fig. 14. A 15 inch driver in a 2 foot^3 box having a Butterworth alignment with a lower -3 dB cutoff frequency of 40 Hz is assumed. The driver parameters are: voice-coil resistance $R_E = 7\ \Omega$, motor product $B\ell = 21.6$ T·m, diaphragm mass $M_{MD} = 197$ grams, suspension resistance $R_{MS} = 8.07$ N·s/m, suspension compliance $C_{MS} = 4.03 \times 10^{-4}$ m/N, and diaphragm piston area $S_D = 0.0707$ m^2. The box parameters are: acoustic mass $M_{AB} = 5.77$ kg/m^4, acoustic resistance $R_{AB} = 1780$ N·s/m^5, and acoustic compliance $C_{AB} = 4.03 \times 10^{-7}$ m^5/N. The resistor R_{AL} is necessary to prevent a floating node in SPICE. Its value was chosen to be 4×10^6 N·s/m^5, which is large enough to be considered an open circuit in the frequency response calculations. This resistor can be considered to model air leaks in the enclosure. The front air-load mass parameters are $M_{A1} = 2.13$ kg/m^4, $R_{A1} = 2540$ N·s/m^5, $R_{A2} = 5760$ N·s/m^5, and $C_{A1} = 1.43 \times 10^{-7}$ m^5/N.

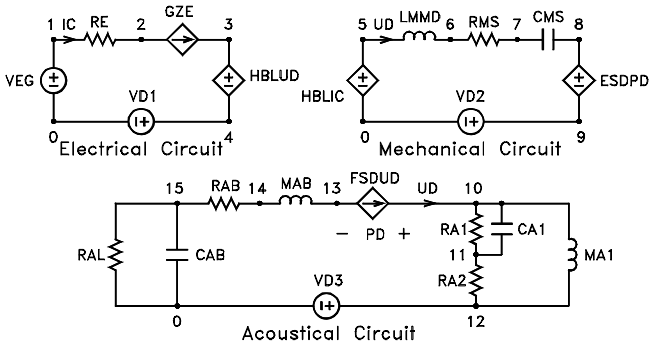

Fig. 14. SPICE circuit for the example simulation.

The SPICE deck for the simulation is given in Table I. The lossy inductor is modeled by the voltage-controlled current source `GZE` between nodes 2 and 3. The current through `GZE`, i.e. through L_E, is given by the voltage `V(2,3)` divided by K`*PWR(S,`n`)`, where `S` is the complex frequency and numerical values must be supplied for K and n. The $+$ sign on the line below `GZE` indicates a continued line. Five values of n between 1.0 and 0.5 were chosen for the simulations. The values are $n = 1$, 0.875, 0.75, 0.625, and 0.5. For $n = 1$, the value $K = 0.001$ was used, corresponding to a lossless inductor with a value of 1 mH. For the other values of n, K was computed so that the SPL curves intersect at the frequency for which $|R_E + K(j\omega)^n| = 3R_E$. This choice was made because it results in an intersection point at a frequency that is approximately the geometric mean of 1 kHz and 10 kHz, i.e. midway between these frequencies on a log scale. The K values are $K = 0.001$, 0.00322, 0.0104, 0.0336, and 0.110.

The on-axis SPL at 1 meter is given by [1]

$$SPL = 20\log\left(\frac{\rho_0 f U_D}{p_{\text{ref}}}\right) \tag{31}$$

where $\rho_0 = 1.18$ kg/m^3 is the density of air, f is the frequency, U_D is the volume velocity output from the diaphragm, and $p_{\text{ref}} = 2 \times 10^{-5}$ Pa is the reference pressure. The SPL can

TABLE I
SPICE DECK FOR THE CLOSED BOX SIMULATION

```
CLOSED-BOX SIMULATION
*ELECTRICAL CIRCUIT
VEG 1 0 AC 1V
RE 1 2 7
GZE 2 3 LAPLACE {V(2,3)}
+={1/(K*PWR(S,n))}
HBLUD 3 4 VD2 21.6
VD1 4 0 AC 0V
*MECHANICAL CIRCUIT
HBLIC 5 0 VD1 21.6
LMMD 5 6 0.197
RMS 6 7 8.07
CMS 7 8 403E-6
ESDPS 8 9 10 13 707E-4
VD2 9 0 AC 0V
*ACOUSTICAL CIRCUIT
FSDUD 13 10 VD2
+707E-4
LMA1 10 12 2.13
RA1 10 11 25400
RA2 11 12 5760
CA1 10 11 0.143E-6
LMAB 13 14 5.77
RAB 14 15 1780
CAB 15 0 403E-9
RAL 15 0 4E6
VD3 12 0 AC 0V
.AC DEC 50 10 1E4
.PROBE
.END
```

be displayed in the PROBE graphics routine of *PSpice* with the line [1]

```
20*LOG10(59E3*FREQUENCY*I(VD3))
```

where `I(VD3)` is the current through the voltage source `VD3`, which is analogous to the volume velocity U_D.

Simulations of the on-axis SPL at 1 meter are shown in Fig. 15. The plots show that the flattest overall response is obtained with the lossless inductor, i.e. the curve labeled $n = 1$. As the losses increase, the flat midband region disappears and the curves become depressed above the fundamental resonance frequency. It is tempting to conclude from this figure that the inductor losses should be minimized for the best response. However, the curves for the lower values of n are calculated for a larger value of K. If K is not increased as n is decreased, the inductor impedance decreases with n and the width of the flat midband region increases.

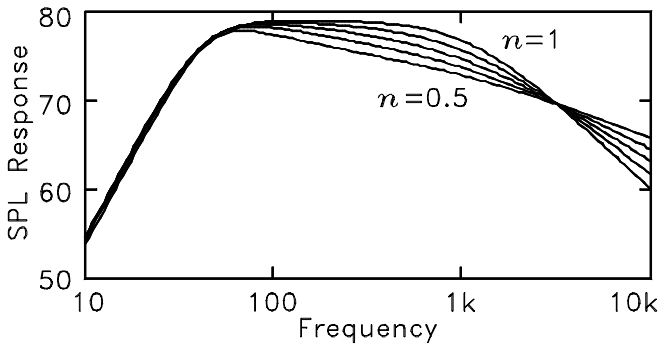

Fig. 15. Simulated SPL responses for five values of n and K.

Corresponding plots for the magnitude of the voice-coil impedance are shown in Fig. 16. This is displayed in the PROBE graphics routine of *PSpice* with the line `1/I(VD1)`, i.e. the source voltage (1 V) divided by the current through the voltage source `VD1`, which is the voice-coil current.

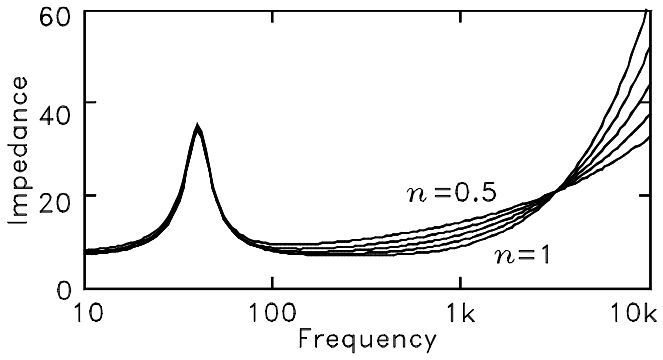

Fig. 16. Simulated voice-coil impedances for five values of n and K.

The author knows of no general relation between K and n so that it is impossible, in general, to predict how changes in one parameter affect the other. However, it has been observed that drivers having lower values of n usually have higher values of K.

VII. Conclusions

It has been shown and experimentally demonstrated that the lossy inductance of a loudspeaker voice coil can be modeled by two parameters K and n. The magnitude of the impedance varies as $K\omega^n$ and the phase is $n\pi/2$. The parameters K and n can be determined from a linear regression analysis of measured voice-coil impedance data. In the author's experience, typical observed values of n lie in the range from 0.6 to 0.7. Changes in the magnet structure of a driver can affect both K and n. Future research for a general analytical relation between these parameters for typical magnet structures could be of value in loudspeaker driver design.

References

[1] W. M. Leach, Jr., *Introduction to Electroacoustics and Audio Amplifier Design*, Second Edition, Revised Printing, (Kendall/Hunt, Dubuque, IA, 2001).

[2] A. N. Thiele, "Loudspeakers in Vented Boxes, Parts I and II," *J. Audio Eng. Soc.*, vol. 19, pp. 382–392 (1971 May); pp. 478–483 (1971 June).

[3] J. Vanderkooy, "A Model of Loudspeaker Impedance Incorporating Eddy Currents in the Pole Structure," *J. Audio Eng. Soc.*, vol. 37, pp. 119–128 (1989 March).

[4] J. R. Wright, "An Empirical Model for Loudspeaker Motor Impedance," *J. Audio Eng. Soc.*, vol. 38, pp. 749–754 (1990 Oct.).

[5] H. W. Bode, *Network Analysis and Feedback Amplifier Design*, (D. Van Nostrand, NY, 1945).

[6] A. E. Fitzgerald and C. Kingsley, *Electric Machinery*, (McGraw-Hill, NY, 1952).

[7] R. H. Small, "Direct-Radiator Loudspeaker System Analysis," *J. Audio Eng. Soc.*, vol. 20, pp. 383-395, (1972 June).

[8] W. M. Leach, Jr., "Computer-Aided Electroacoustic Design with SPICE," *J. Audio Eng. Soc.*, vol. 39, pp. 551–563, (1991 July/Aug.).